

Adaptive-Quadrature Fluctuation-Splitting Schemes for the Euler Equations

Hiroaki Nishikawa *and Philip L. Roe †

W. M. Keck Foundation Laboratory for Computational Fluid Dynamics

Department of Aerospace Engineering

The University of Michigan, Ann Arbor, MI 48109

In this paper, we consider fluctuation-splitting schemes that can capture an isolated shock over a suitably-oriented single triangular element and also recognize a rarefaction. A particular focus is on the evaluation of the fluctuation (or the cell-residual): a one-parameter-family quadrature rule is employed to evaluate the fluctuation, which endows the fluctuation with a wave recognition capability. The parameter value is chosen based on the nature of the nonlinear wave passing through the element, and then the resulting fluctuation is distributed to the nodes. This strategy, combined with various distribution schemes, defines a family of adaptive-quadrature fluctuation-splitting schemes. Results demonstrate the superior ability of the new schemes in handling nonlinear waves compared with standard fluctuation-splitting schemes which cannot capture shocks over a single element and also admits non-physical shocks unless some kind of entropy-fix is incorporated.

I. Introduction

Fluctuation-splitting(or residual-distribution) schemes are multidimensional upwinding schemes that have been developed mainly for unstructured triangular/tetrahedral meshes. This scheme is based on cell residual (fluctuation) with variables stored at nodes, and consists of two steps: first compute the flux balance (fluctuation/residual) over an element, and then distribute it to the nodes of the element to bring changes to the nodal variables. Note that both steps are based on complete elements, not on lower-dimensional components such as faces or edges (as in the finite-volume methods). This elementwise operation enables multidimensional physics to be directly taken into account, and this is one of the advantages of the fluctuation-splitting schemes over the finite-volume schemes.

Despite many superior features over the conventional finite-volume schemes, however, existing fluctuation-splitting schemes cannot capture a shock over a single element and also admits non-physical shocks. A form of entropy-fix has been reported by Sermeus and Deconinck.¹ Their method is based on modifying the wave speeds in the distribution matrices. This generalizes the one-dimensional entropy fix of Harten and Hyman.² In this work, we take a different approach and develop a method that can compute entropy-satisfying expansions as well as capture a shock over a single element, focusing on the evaluation of the fluctuation. In the development of the fluctuation-splitting schemes, the effort has been put mainly in the development of the distribution coefficients while the fluctuation itself has been evaluated exclusively with the conservative linearization. Some recent works focus on arbitrary quadrature rules to evaluate the fluctuation, in order to make it possible to apply the fluctuation-splitting schemes to general systems of equations for which the exact linearization may not be possible,³ or to achieve higher order accuracy.^{4,5} This paper explores yet another possibility of using quadrature formulas for fluctuations to control the wave recognition property of the fluctuation-splitting schemes.

For the Euler equations, a one-parameter family of quadrature rules is employed to evaluate the fluctuation. The resulting fluctuation is given flexibility to handle different kinds of flow features by the freedom to choose the parameter. The parameter value is chosen based on the nature of the nonlinear wave that is

*Research Fellow, Member AIAA

†Professor, Fellow AIAA

present inside the element. In order to detect such waves, a multidimensional way of detecting nonlinear waves is also given.

Section 2 gives an overview of the fluctuation-splitting schemes with a particular emphasis on those that can distribute the fluctuation evaluated by a general quadrature rule. Section 3 describes the quadrature rule for the fluctuation and its properties. Section 4 discusses a way to detect shocks/expansions and to assign the parameter. Section 5 shows results, and Section 6 concludes the paper.

II. Fluctuation-Splitting Schemes

We consider solving sets of conservation laws of the form

$$\mathbf{u}_t + \partial_x \mathbf{f} + \partial_y \mathbf{g} = 0 \quad (1)$$

where \mathbf{u} is a vector of conservative variables, in the domain divided into a set of triangles $\{T\}$. In the fluctuation-splitting schemes, the first step is to compute the fluctuation Φ^T for all triangles $T \in \{T\}$,

$$\Phi^T = - \int_T \mathbf{u}_t dV = \int_T (\partial_x \mathbf{f} + \partial_y \mathbf{g}) dV \quad (2)$$

which is evaluated by a certain quadrature rule. This is the focus of this paper and will be discussed in details in the next section. The second step is to distribute the fluctuation, in a way that reflects multidimensional physics, to the nodes to suggest changes in the nodal variables. This results in the following update formula for a solution at node j ,

$$\mathbf{u}_j^{n+1} = \mathbf{u}_j^n - \frac{\Delta t}{V_j} \sum_{T \in \{T_j\}} \Phi_i^T \quad (3)$$

where

$$\Phi_i^T = \mathcal{B}_j^T \Phi^T \quad (4)$$

and $\{T_j\}$ is a set of triangles that shares the node j , $\Delta t = t^{n+1} - t^n$ is a (local or global) timestep, V_j is the volume of the median dual control volume, and \mathcal{B}_j^T is the distribution matrix that assigns the fraction of the fluctuation sent to the node j within the triangle T . We consider only conservative schemes characterized by

$$\sum_j \mathcal{B}_j^T = I \quad (5)$$

where I is the identity matrix. Various such distribution matrices are available. They are all based on the so-called inflow matrix and its characteristic decomposition defined by

$$\mathbf{K}_i = \frac{1}{2} (\mathbf{A}, \mathbf{B}) \cdot \mathbf{n}_i, \quad \mathbf{K}_i^\pm = \mathbf{R}_i \Lambda_i^\pm (\mathbf{R}_i)^{-1} \quad (6)$$

where $\mathbf{A} = \frac{\partial \mathbf{f}}{\partial \mathbf{u}}$, $\mathbf{B} = \frac{\partial \mathbf{g}}{\partial \mathbf{u}}$, $\mathbf{n}_i = (n_i^x, n_i^y)$ is the scaled inward normal vector opposite to the node i , the columns of \mathbf{R}_i are the right eigenvectors of \mathbf{K}_i , and Λ is the corresponding diagonal matrix of the eigenvalues. In this work, we use the nonlinear matrix N-scheme of Csik et. al.³

$$\Phi_i^T = \mathbf{K}_i^+ (\mathbf{u}_i - \mathbf{u}_{in}) \quad (7)$$

where

$$\mathbf{u}_{in} = - \left(\sum_i \mathbf{K}_i^- \right)^{-1} \left(\sum_i \mathbf{K}_i^+ \mathbf{u}_i - \Phi^T \right) \quad (8)$$

and the matrix LDA scheme,

$$\mathcal{B}_j^T = \mathbf{K}_j^+ \left(\sum_i \mathbf{K}_i^+ \right)^{-1}. \quad (9)$$

The former is used when the monotonicity is important while the latter is used when the linearity preserving property is important. The primary reason for these, however, is that both of these schemes can distribute the fluctuation independently of how it is evaluated. We need this property because we are going to compute the fluctuation in an adaptive manner.

Note that there exist typically twice as many triangles as nodes in a triangular mesh, and hence there are twice as many fluctuations as nodal solutions. This results in a highly overdetermined problem, and therefore the fluctuation Φ^T cannot be made to vanish everywhere. To equalize the number of unknowns and the number of equations, we define a nodal residual at every node by taking a weighted average of the fluctuations over the triangles that share the node. However, it is reasonable to assume that the fluctuations are small at convergence, and usually they are. In this sense, the distribution step may be thought of as minimizing the fluctuations by rendering appropriate changes to the nodal variables. In fact, this is precisely the case for the least-squares scheme in which \mathcal{B}_j^T is the negative gradient of the fluctuation with respect to the nodal variables, and this also applies to the LDA scheme that is known to be a variant of the least-squares scheme. Based on this particular viewpoint, in this work, we design the fluctuation-splitting schemes in terms of how the fluctuation is defined rather than how to distribute it.

III. Quadrature Formula

Consider conservation laws for which each component of the fluxes is a bilinear function of the components of a certain set of variables \mathbf{w} ,

$$\mathbf{f}(\mathbf{w}) = \mathbf{w}^t \mathbf{C} \mathbf{w}, \quad \mathbf{g}(\mathbf{w}) = \mathbf{w}^t \mathbf{D} \mathbf{w} \quad (10)$$

where \mathbf{C} and \mathbf{D} are constant symmetric third-order tensors, and the superscript t denotes the transpose. This structure includes the Euler equations of compressible inviscid flow if \mathbf{w} is taken to be Roe's parameter vector.⁶ Note that we have

$$\mathbf{A}_w(\mathbf{w}) = \frac{\partial \mathbf{f}}{\partial \mathbf{w}}(\mathbf{w}) = 2 \mathbf{w}^t \mathbf{C} \quad (11)$$

$$\mathbf{B}_w(\mathbf{w}) = \frac{\partial \mathbf{g}}{\partial \mathbf{w}}(\mathbf{w}) = 2 \mathbf{w}^t \mathbf{D} \quad (12)$$

Fluctuation over a triangle defined by the vertices 1-2-3 is

$$\Phi_{123} = \iint_{123} [\partial_x \mathbf{f}(\mathbf{w}) + \partial_y \mathbf{g}(\mathbf{w})] dx dy \quad (13)$$

$$= \oint_{123} [\mathbf{f}(\mathbf{w}) dy - \mathbf{g}(\mathbf{w}) dx]. \quad (14)$$

Along each edge, there is a class of simple quadrature formulas⁷ defined by

$$\begin{aligned} \mathbf{F}_{12} &= \int_1^2 \mathbf{f}(\mathbf{w}) dy = \int_1^2 \mathbf{w}^t \mathbf{C} \mathbf{w} dy \\ &= (y_2 - y_1) \left[\mathbf{w}_1^t \mathbf{C} \mathbf{w}_2 + \frac{\alpha}{2} (\mathbf{w}_2 - \mathbf{w}_1)^t \mathbf{C} (\mathbf{w}_2 - \mathbf{w}_1) \right] \end{aligned} \quad (15)$$

where α is a parameter to be assigned. Clearly, the formula is 2nd-order accurate for any α . If we assume, although we do not have to, that the same value is assigned to α for all edges, then by collecting contributions from all edges, and arranging, we arrive at

$$\begin{aligned} \Phi_{123} &= \frac{1}{2} \sum_i [\mathbf{A}_w(\tilde{\mathbf{w}}_\alpha) n_i^x + \mathbf{B}_w(\tilde{\mathbf{w}}_\alpha) n_i^y] \mathbf{w}_i \\ &\quad - \frac{\beta}{2} [(\mathbf{A}_w(\mathbf{w}_3) n_2^x + \mathbf{B}_w(\mathbf{w}_3) n_2^y) \mathbf{w}_1 \\ &\quad \quad + (\mathbf{A}_w(\mathbf{w}_1) n_3^x + \mathbf{B}_w(\mathbf{w}_1) n_3^y) \mathbf{w}_2 \\ &\quad \quad + (\mathbf{A}_w(\mathbf{w}_2) n_1^x + \mathbf{B}_w(\mathbf{w}_2) n_1^y) \mathbf{w}_3] \end{aligned} \quad (16)$$

where

$$\tilde{\mathbf{w}}_\alpha = \frac{\alpha}{2} (\mathbf{w}_1 + \mathbf{w}_2 + \mathbf{w}_3), \quad \beta = \frac{3}{2} \left(\frac{2}{3} - \alpha \right). \quad (17)$$

It follows immediately from this that the choice $\alpha = 2/3$ corresponds to the so-called conservative linearization,⁸ which has been almost exclusively the choice of previous investigations.

Suppose that two of the nodes of a triangle happen to be in the same state, say $\mathbf{w}_1 = \mathbf{w}_2 = \mathbf{w}_c$. Then, we have

$$\begin{aligned}\Phi_{123} = & (y_3 - y_2) \left[\mathbf{w}_2^t \mathbf{C} \mathbf{w}_3 + \frac{\alpha}{2} (\mathbf{w}_3 - \mathbf{w}_2)^t \mathbf{C} (\mathbf{w}_3 - \mathbf{w}_2) \right] \\ & + (y_1 - y_3) \left[\mathbf{w}_1^t \mathbf{C} \mathbf{w}_3 + \frac{\alpha}{2} (\mathbf{w}_1 - \mathbf{w}_3)^t \mathbf{C} (\mathbf{w}_1 - \mathbf{w}_3) \right] \\ & + (y_2 - y_1) \mathbf{w}_1^t \mathbf{C} \mathbf{w}_2 \\ & - (x_3 - x_2) \left[\mathbf{w}_2^t \mathbf{D} \mathbf{w}_3 + \frac{\alpha}{2} (\mathbf{w}_3 - \mathbf{w}_2)^t \mathbf{D} (\mathbf{w}_3 - \mathbf{w}_2) \right] \\ & - (x_1 - x_3) \left[\mathbf{w}_1^t \mathbf{D} \mathbf{w}_3 + \frac{\alpha}{2} (\mathbf{w}_1 - \mathbf{w}_3)^t \mathbf{D} (\mathbf{w}_1 - \mathbf{w}_3) \right] \\ & - (x_2 - x_1) \mathbf{w}_1^t \mathbf{D} \mathbf{w}_2.\end{aligned}\tag{18}$$

Note that the terms proportional to α have identically vanished on the edge 1-2, i.e. the fluctuation is independent of α on the edge along which the solution value is constant. The fluctuation further simplifies to

$$\Phi_{123} = \bar{\mathbf{w}}_\alpha^t [\Delta y \mathbf{C} - \Delta x \mathbf{D}] (\mathbf{w}_c - \mathbf{w}_3)\tag{19}$$

where $\Delta() = ()_2 - ()_1$, and

$$\bar{\mathbf{w}}_\alpha = \frac{2 - \alpha}{2} \mathbf{w}_c + \frac{\alpha}{2} \mathbf{w}_3.\tag{20}$$

Now, taking $\alpha = 1$, this discretization becomes precisely the Rankine-Hugoniot relation, with S being the slope of the shock,

$$S \Delta \mathbf{f} - \Delta \mathbf{g} = \left(\frac{\mathbf{w}_c + \mathbf{w}_3}{2} \right)^t (S \mathbf{C} - \mathbf{D}) \Delta \mathbf{w} = 0\tag{21}$$

provided the shock is parallel to the edge 1-2, i.e. $S = \Delta y / \Delta x$. This was originally shown in,⁷ but it was not explicitly stated that this property is independent of α for the edge parallel to the shock. This result shows that a shockwave can be spanned by a single element, and therefore captured exactly, only if $\alpha = 1$. It also shows that the capturing element can be arbitrarily narrow, so that the shock can be captured with arbitrarily high resolution. Of course, these properties are not fully exploitable unless the mesh is made adaptive, and this is an aspect on which we are not yet ready to report. Although equation (21) coincides with the Rankine-Hugoniot condition when $\alpha = 1$, it does not distinguish the direction of the jump and hence admits expansion shocks. However, the nonphysical shocks can be avoided simply by taking a different value of α . This parameter α is in fact closely related to the entropy production. A one-dimensional analysis for Burgers' equation shows that the entropy function is conserved with $\alpha = \frac{2}{3}$ and reduced with $\alpha < \frac{2}{3}$, thus ensuring physical solutions.⁹

IV. Adaptive Quadrature

To choose α for a particular element, we need to know if the element is in a shock or in a rarefaction or away from such nonlinear waves. For this purpose, we use the divergence of the steady-characteristic speeds, originally proposed in,⁷

$$\int_T \operatorname{div} \bar{\lambda}^k \, dx dy = \frac{1}{2} \sum_i \bar{\lambda}_i^k \cdot \mathbf{n}_i\tag{22}$$

where $\bar{\lambda}^k$ has been assumed to vary linearly over the element and $\bar{\lambda}_i^k$ is the k -th steady-characteristic speed vector evaluated at a node i . For the sake of convenience, in this work, we define the following

$$\Delta_k = \frac{\sum_i \bar{\lambda}_i^k \cdot \mathbf{n}_i}{\sum_i |\bar{\lambda}_i^k| |\mathbf{n}_i|}\tag{23}$$

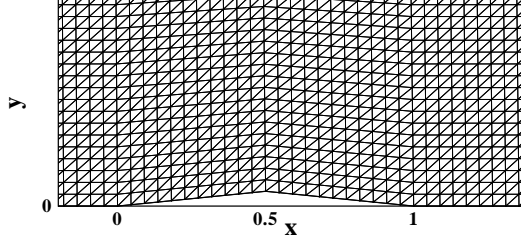


Figure 1. A blow-up of the grid used for the first test case.

in which the quantity in the denominator has been introduced to normalize Δ_k such that

$$-1 \leq \Delta_k \leq 1 \quad (24)$$

We know that a shock is present if this quantity is negative (converging characteristic field) and a rarefaction presents if positive (diverging characteristic field). This leads us to dividing the range into three parts,

$$\begin{cases} -1 \leq \Delta_k \leq -\delta & \rightarrow \text{Shock} & \rightarrow \alpha = 1 \\ -\delta < \Delta_k < \delta & \rightarrow \text{Uniform} & \rightarrow \alpha = 2/3 \\ \delta \leq \Delta_k \leq 1 & \rightarrow \text{Rarefaction} & \rightarrow \alpha = 0 \end{cases} \quad (25)$$

We experimentally found that it worked well with $\delta \approx 10^{-3}$. For the Euler equations, there are two possible nonlinear waves in supersonic flows, whose characteristic speeds are given by

$$\vec{\lambda}^1 = (u\beta - v, v\beta + u) \quad (26)$$

$$\vec{\lambda}^2 = (u\beta + v, v\beta - u) \quad (27)$$

where $\beta = \sqrt{M^2 - 1}$. Note that

$$\text{div} \vec{\lambda}^1 = \text{div}(\beta \mathbf{q}) - \omega \quad (28)$$

$$\text{div} \vec{\lambda}^2 = \text{div}(\beta \mathbf{q}) + \omega \quad (29)$$

where $\mathbf{q} = (u, v)$ and $\omega = \partial_x v - \partial_y u$. This means that we detect and distinguish waves using a combination of the divergence and the vorticity of the flowfield. Note also that we have

$$\left(\text{div} \vec{\lambda}^1\right)^2 + \left(\text{div} \vec{\lambda}^2\right)^2 = \left(\text{div}(\beta \mathbf{q})\right)^2 + \omega^2. \quad (30)$$

To detect a dominant wave, we first compute Δ_k for $k = 1, 2$, take the larger of the two in magnitude, and then use (25) to determine the value of α for the element. We remark that we use $\alpha = 2/3$ if all of the nodes of an element are in a subsonic flow for which the acoustic system is elliptic and there exist no characteristics. Also, note that we set $\alpha = 1$ for the elements with both subsonic and supersonic nodes as it indicates the presence of a strong shock running across the element.

The resulting method is not conservative because α is assigned element-wise and therefore line integrals do not cancel over an edge shared by two triangles with different α . This can be fixed fairly easily by unifying the value of α over such an edge whenever the line integral would be evaluated with different α in the adjacent elements. In this work, we set $\alpha = 1$ if either of the two α 's is 1, and set $\alpha = 0$ if either of the two α 's is 0. With this fix, the method becomes conservative.

V. Results

The first test case is a supersonic flow over a triangular bump at Mach number of 1.69. The grid is a regular triangular grid of size 100x50 nodes. All cases were computed with the nonlinear matrix N-scheme

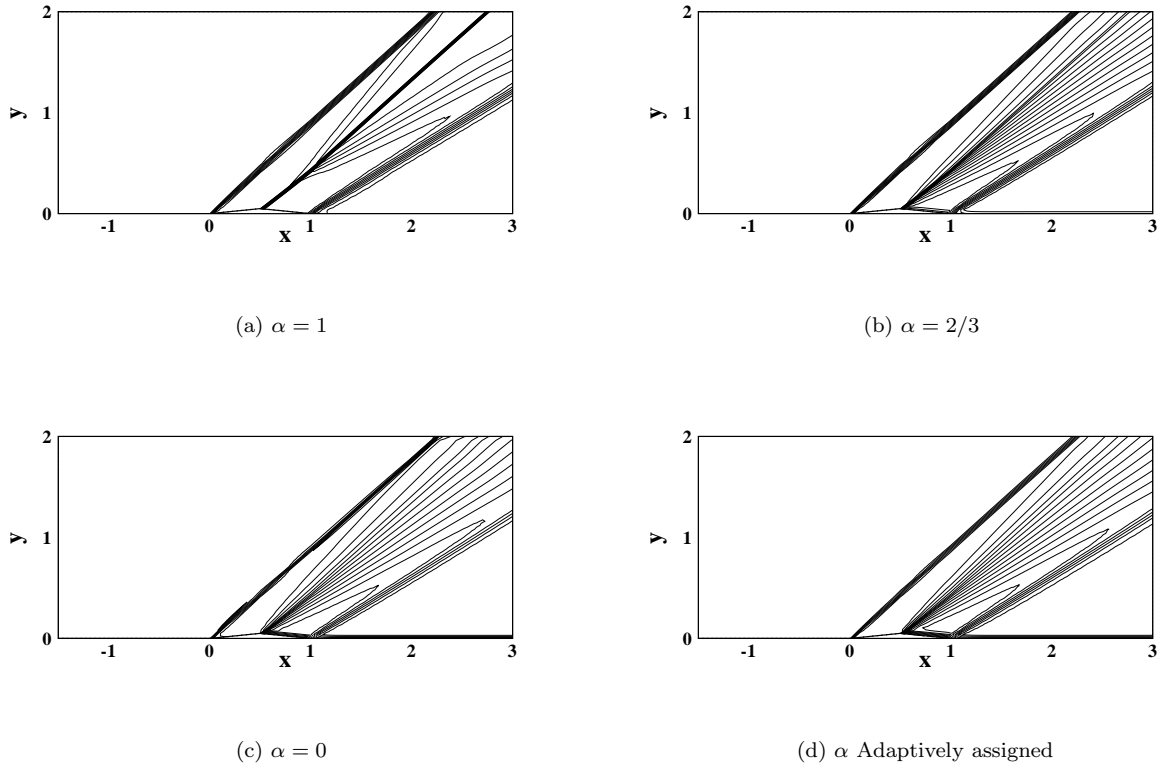


Figure 2. Results by the nonlinear N-Scheme with various types of fluctuations.

(7) with the distribution matrix evaluated at the arithmetic average of the parameter vector over a triangle. Figures 2-(a) to 2-(c) show the Mach contours for cases with $\alpha = 1$, $\alpha = \frac{2}{3}$, $\alpha = 0$ respectively, for all triangles. It is clear from these that the choice of $\alpha = 1$ results in an expansion shock, $\alpha = \frac{2}{3}$ still suffers from an expansion shock although weaker, and $\alpha = 0$ produces a correct expansion fan. Figure 2-(d) shows the result with the adaptive choice of α with $\delta = 3.0E - 03$. The expansion fan is as cleanly computed as the one with $\alpha = 0$ everywhere. See also Figures 3-(a) to 3-(c) which show the plots of Mach number along a line passing over the waves at $y = 0.65$, sampled from the corresponding results in Figures 2. We remark that the shock/expansion detection mechanism works very well, accurately identifying elements in shocks and a rarefaction as can be seen in Figure 8.

The second test case is a grid-aligned oblique shock wave at a corner. The domain is taken as a square. With the bottom boundary taken as a wall and the left as a deflected supersonic inflow, an oblique shock wave is generated at the bottom left corner. In this test, a flow with Mach 1.52567142 inclined at -10° is chosen in order to generate a shock at 45° from the bottom of the domain. For this test, the LDA scheme (7) was used. Figure 5 shows the computational grid which is based on a 10×10 Cartesian grid with diagonals inserted so as to make the grid aligned with the oblique shock. Two methods are compared here: the LDA with ($\alpha = \frac{2}{3}$) and with adaptive α , starting from a common initial solution such that the inflow condition is given everywhere initially and a steady state solution is computed. Figure 6 shows the entropy contours for the LDA scheme with the conservative linearization ($\alpha = \frac{2}{3}$). The solution is not particularly clean, but this is not surprising for non-monotone schemes such as the LDA and for such a coarse mesh. Figure 7 shows the entropy contours obtained by the same LDA scheme but with α adaptively assigned for the fluctuation. The solution is exact with no spurious entropy whatsoever. As seen in Figure 8 where the value of α is plotted elementwise, the elements in the shock have been perfectly detected and given $\alpha = 1$. And because these elements have a side parallel to the shock, their fluctuations completely vanish, satisfying the Rankine-Hugoniot relation.

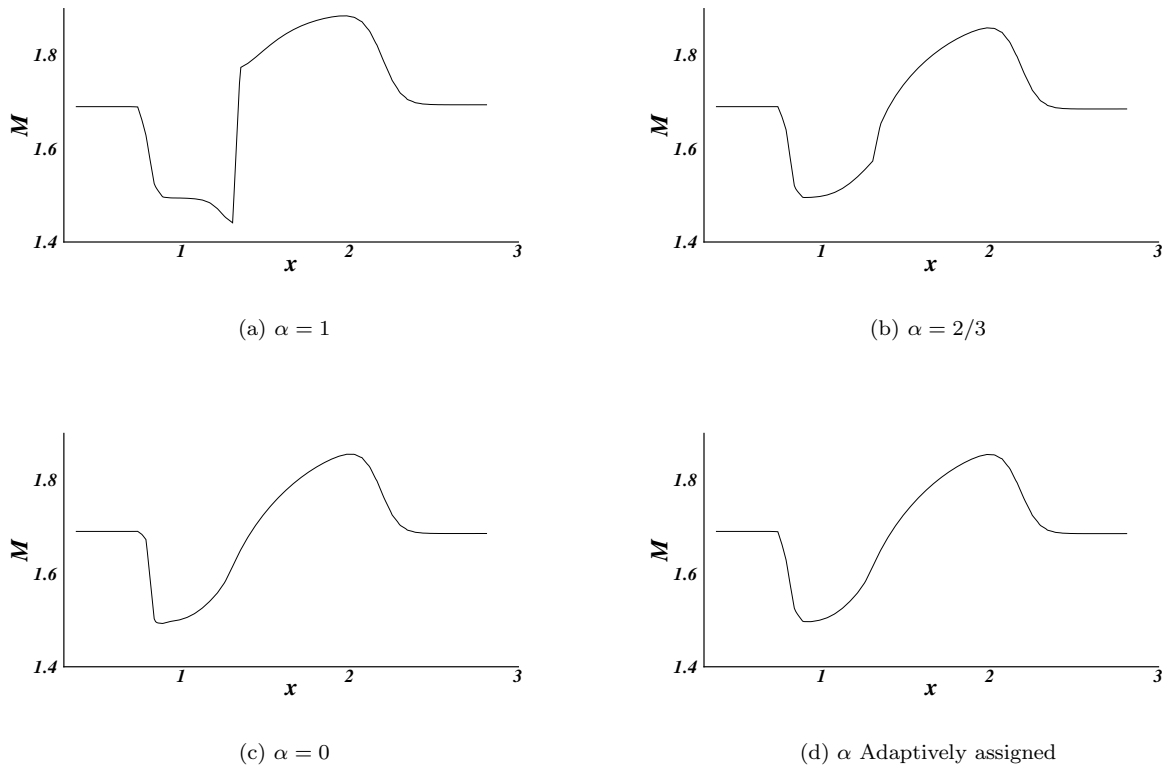


Figure 3. Plots of Mach number along a line at $y = 0.65$.

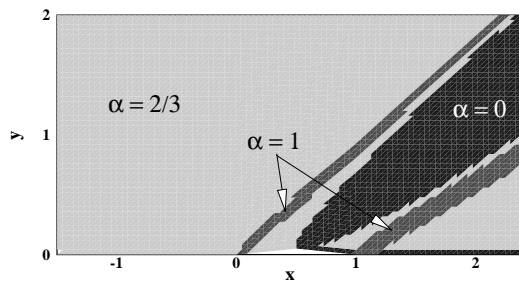


Figure 4. Elementwise distribution of α over the domain.

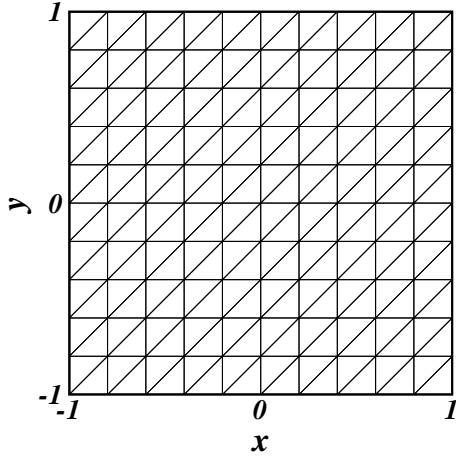


Figure 5. Grid for the oblique-shock test case.

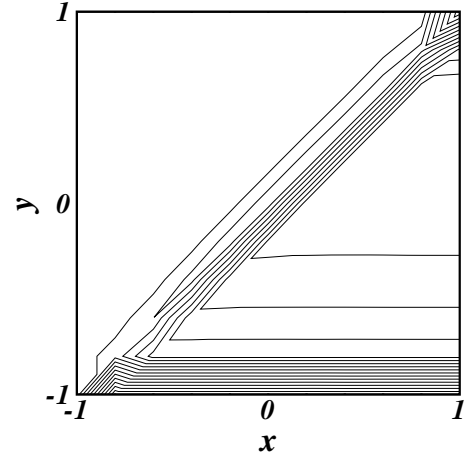


Figure 6. Entropy contours. The LDA-Scheme with $\alpha = 2/3$.

VI. Concluding Remarks

This paper has shown that the fluctuation-splitting schemes can be designed to recognize shocks over a single element as well as to avoid nonphysical shocks by evaluating the fluctuation in an adaptive manner. Results show significant improvement over the conventional schemes. Also, the nonlinear wave detection algorithm has shown to work so well that it could be used alone for other purposes, for example, to identify regions for grid refinement.

In this work, we first assigned the parameter α for all elements and then computed the fluctuations. These two processes may be combined into a single-loop-process to improve the efficiency. It would also be possible to assign α edge-wise rather than element-wise because α does not have to be the same within the element and it would eliminate the need to fix the conflicting α on edges for conservation.

For shock capturing, the method would work best with an adaptive grid method as the single-element shock capturing is possible only when one of the edges is aligned with the shock. One strategy is to minimize the fluctuations with respect to nodal solutions as well as coordinates, which in fact was already demonstrated for Burgers' equation in.⁷ We remark that we can apply the grid movement in only limited regions by taking advantage of the excellent capability of the wave detection algorithm.

Acknowledgments

This work has been sponsored by the Space Vehicle Technology Institute, under grant NCC3-989, one of the NASA University Institutes, with joint sponsorship from the Department of Defense. Appreciation is expressed to Claudia Meyer, Mark Klemm and Harry Cikanek of the NASA Glenn Research Center, and to Dr. John Schmisser and Dr. Walter Jones of the Air Force Office of Scientific Research.

References

- ¹Sermeus, K. and Deconinck, H., "An Entropy Fix for Multi-Dimensional Upwind Residual Distribution Schemes," *Computers and Fluids*, Vol. 34, 2005, pp. 617–640.
- ²Harten, A. and Hyman, J. M., "Self-Adjusting Grid Methods for One-Dimensional Hyperbolic Conservation Laws," *JCP*, Vol. 50, 1983, pp. 235–269.
- ³Csik, A., Ricchiuto, M., and Deconinck, H., "A Conservative Formulation of the Multidimensional Upwind Residual Distribution Schemes for General Nonlinear Conservation Laws," *JCP*, Vol. 179, 2002, pp. 286–312.
- ⁴Caraeni, D. and Fuchs, L., "Compact Third-Order Multidimensional Upwind Scheme for Navier-Stokes Simulations,"

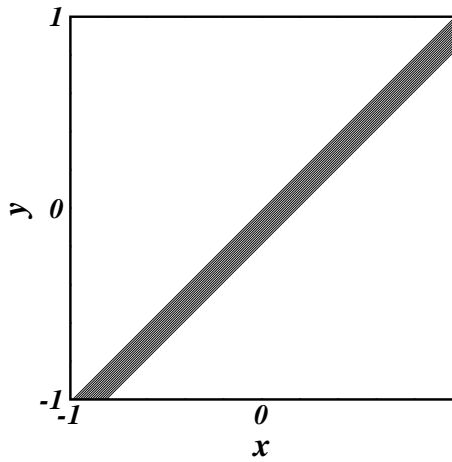


Figure 7. Entropy contours. The LDA-Scheme with adaptive α .

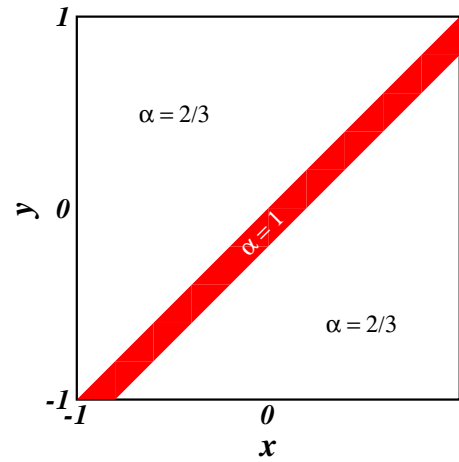


Figure 8. Elementwise distribution of α over the domain.

Theoretical and Computational Fluid Dynamics, Vol. 15, 2002, pp. 373–401.

⁵Nishikawa, H., Rad, M., and Roe, P., “A Third-Order Fluctuation-Splitting Scheme That Preserves Potential Flow,” *15th AIAA Computational Fluid Dynamics Conference*, AIAA Paper 01-2595, Anaheim, 2001.

⁶Roe, P. L., “Approximate Riemann Solvers, Parameter Vectors and Difference Schemes,” *JCP*, Vol. 43, 1981, pp. 357–372.

⁷Nishikawa, H., Rad, M., and Roe, P., “Grids and Solutions from Residual Minimisation,” *Computational Fluid Dynamics 2000*, Springer-Verlag, 2000.

⁸Deconinck, H., Roe, P. L., and Struijs, R., “A Multi-Dimensional Generalization of Roe’s Flux Difference Splitter for the Euler Equations,” *Computers and Fluids*, Vol. 43, 1981, pp. 357–372.

⁹Roe, P. L. and Nishikawa, H., “Adaptive Grid Generation by Minimising Residuals,” *International Journal for Numerical Methods in Fluids*, Vol. 40, 2002, pp. 121–136.